Can. J. Remote Sensing, Vol. 35, No. 6, pp. 523–533, 2009

Disturbance capture and attribution through the integration of Landsat and IRS-1C imagery

Benjamin P. Stewart, Michael A. Wulder, Gregory J. McDermid, and Trisalyn Nelson

Abstract. A primary activity required to support sustainable forest management is the detection and mitigation of forest disturbances. These disturbances can be planned, through urbanization and harvesting, or unplanned, through insect infestations or fire. Detection and characterization of disturbance types are important, as different disturbances have different ecological effects and may require unique managerial responses. As such, it is necessary for forest managers to have as complete and current information as possible to support decision making. In this study, we developed a framework to automatically detect and label disturbances derived from remotely sensed images. Disturbances were detected through traditional image differencing of medium-resolution imagery (Landsat-7 Enhanced Thematic Mapper Plus (ETM+), resampled to 30 m) but were refined and augmented through comparison with edge features extracted from high spatial resolution satellite imagery (Indian Remote Sensing (IRS) satellite 1C panchromatic imagery, resampled to 5 m). By incorporating spectral information, derived composite band values (tasselled cap transformations), spatial and contextual information, and secondary datasets, we were able to capture and label disturbance features with a high level of overall agreement (91%). Areal features, such as harvest areas, are captured and labelled more reliably than linear features such as roads, with 92% and 72% agreement when compared with control data, respectively. By incorporating rule-based disturbance attribution with remote sensing change detection, we envision the update of land cover databases with reduced human intervention, aiding more rapid data integration and opportunities for timely managerial responses.

Résumé. La détection et l'atténuation des perturbations dans une forêt constituent une étape essentielle pour assurer la gestion durable de la forêt. Ces perturbations peuvent être planifiées, comme dans le cas de l'urbanisation et de l'exploitation forestière ou encore, non planifiées suite à des infestations par les insectes ou des incendies. La détection et la caractérisation des divers types de perturbations sont importantes étant donné que ces différentes perturbations entraînent des effets écologiques différents et peuvent exiger des réponses qui leur sont propres en termes de gestion. Ainsi, il est nécessaire pour les gestionnaires de la forêt de disposer de l'information la plus complète et la plus à jour possible pour soutenir le processus de prise de décision. Dans cette étude, on développe une méthodologie pour détecter et étiqueter automatiquement les perturbations dérivées des images de télédétection. Les perturbations ont été détectées en utilisant la méthode traditionnelle de différenciation d'images à moyenne résolution (images ETM+ (« Enhanced Thematic Mapper Plus ») de Landsat-7, ré-échantillonnées à 30 m), quoique celles-ci aient été raffinées et améliorées par le biais d'une comparaison avec les caractéristiques de contours extraites d'images satellite à haute résolution spatiale (images panchromatiques du satellite IRS-1C (« Indian Remote Sensing satellite 1C »), ré-échantillonnées à 5 m). En intégrant l'information spectrale, les valeurs des bandes composites dérivées (espace indiciel transformé-TCT), l'information spatiale et contextuelle ainsi que des ensembles secondaires de données, il a été possible de capturer et d'étiqueter les caractéristiques des perturbations avec un niveau global de concordance élevé (91 %). Les caractéristiques spatiales, comme la surface des zones de coupe, sont capturées et étiquetées de façon plus fiable que les caractéristiques linéaires telles que les routes, avec une concordance de 92 % et de 72 % respectivement comparativement aux données de contrôle. En intégrant l'attribution des perturbations obtenue à l'aide d'un système à base de règles avec les résultats de la détection des changements par télédétection, on envisage de réaliser la mise à jour des bases de données du couvert avec une intervention humaine minimale facilitant ainsi l'intégration plus rapide des données tout en accroissant les capacités de réponse des gestionnaires à court terme.
[Traduit par la Rédaction]

Introduction

As demands placed on the environment by anthropogenic activities continue to increase, society is growing increasingly aware of the impacts such activities have on the environment (McFarlane and Boxall, 2000; Schneider et al., 2003; Nielsen et al., 2004). To effectively manage natural resources, land managers require timely information quan-

Received 10 September 2009. Accepted 7 December 2009. Published on the Web at http://pubservices.nrc-cnrc.ca/cjrs on 4 June 2010.

B.P. Stewart and T. Nelson. Department of Geography, University of Victoria, PO Box 3050, Station CSC, Victoria, BC V8W 3P5, Canada.
M.A. Wulder.[1] Pacific Forestry Centre, Canadian Forest Service, Natural Resources Canada, Victoria, BC V8Z 1M5, Canada.
G.J. McDermid. Department of Geography, University of Calgary, Calgary, AB T2N 1N4, Canada.

[1]Corresponding author (e-mail: mwulder@nrcan.gc.ca).

tifying the location, size, and cause of environmental disturbance related to the extraction of natural resources (e.g., mining and forestry) and human development (Hayes and Sader, 2001; Desclee et al., 2006). Although the detection of disturbances is integral to proper ecosystem management, understanding the underlying cause of the change is often equally important because different disturbance types often yield different ecologic effects (Zager et al., 1983; Archibald et al., 1987; Mace et al., 1996).

Indeed, spatially explicit disturbance detection is of particular importance to natural resource management. Remotely sensed data are frequently employed to develop spatially explicit data identifying areas experiencing environmental change (Coppin and Bauer, 1996; Coppin et al., 2004; Radke et al., 2005). Many remote sensing based change detection approaches are considered operational, depending on the type of imagery used and the disturbances being investigated (Cohen et al., 1998; Woodcock et al., 2001). Medium spatial resolution satellite sensors (i.e., those with pixels sided 10–100 m) capture land cover and disturbance information at a spatial scale relevant to human activities. Further, medium spatial resolution sensors often have large image extents that reduce the need for multi-image mosaicking and normalization which is particularly useful for monitoring of environmental change across large areas (Wulder et al., 2008). Landsat data, for example, are commonly used to detect and monitor ecosystem change and have proven useful for the detection of areal disturbances (such as forest harvesting and fires) (e.g., Cohen et al., 2002). However, detecting changes that are linear in nature (e.g., road construction) is often challenging with medium spatial resolution data due to the lack of requisite spatial precision (Klang, 1998; Zhang et al., 2002; Linke et al., 2008).

Detecting and labelling disturbances (hereafter termed change attribution) are also integral aspects of change modelling. Coppin et al. (2004) describe change attribution as a process separate from disturbance detection; the categorization of disturbances should be considered an independent procedure whereby an attribution framework can function regardless of the change detection method. Change attribution is often performed manually, ultimately limiting the timeliness and availability of information. Furthermore, manual processing of remotely sensed imagery is a subjective process that can result in large inter-interpreter differences in derived products (Hyyppa et al., 2000; Culvenor, 2003). Change attribution via remote sensing has focused primarily on employing information quantifying the spectral responses related to various types of change (Fung and LeDrew, 1988; Häme et al., 1998). Spectral information is useful; however, remotely sensed data contain additional information that may improve change attribution. For example, metrics quantifying the shape of image features (e.g., area, perimeter, elongatedness) have been successfully employed to improve remote sensing based land cover classifications (Lewis et al., 1997; Frohn, 2006). As shape is often related to disturbance type, these metrics are expected to aid in the attribution of change (Ludeke et al., 1990).

A change detection and attribution framework integrating spectral reflectance values, contextual information, and shape-based attributes could aid in the quantification of environmental change and ultimately lead to improved management responses and change mitigation procedures. The current study demonstrates a novel approach for the automated detection and categorical attribution of remotely sensed disturbance features, with a specific focus on detecting and attributing changes in forest cover related to timber harvesting, oil and gas exploration (i.e., well-site development), and transportation development (i.e., road construction). This is achieved via a three-step data-processing procedure. In the first step, forest disturbances are extracted using standard change detection methodology applied to medium spatial resolution imagery (Landsat). Second, higher spatial resolution Indian Remote Sensing (IRS-1C) imagery is used to extract edges to define and extract linear features. Third, spatial and spectral characteristics of remotely sensed change events are integrated with logical rules to produce disturbance-type labels (e.g., harvest, well site, and road). Through this three-step process, we build on existing knowledge and demonstrate an enhancement to current change detection methods with change feature augmentation (possible through integration with higher spatial resolution imagery) and attribution protocols.

Background

Extending a classification to include attributes concerning shape adds additional information that is not readily available from spectral reflectance data alone. Shape indices can be grouped into *single*- and *multiple*-parameter indices. Single-parameter indices are conceptually simpler but are often insufficiently complex to differentiate features. Examples of single-parameter indices include area, perimeter, and edge count. Multiple-parameter indices are more complex. However, this complexity can lead to more involved classification solutions (Wentz, 1997).

Quantitative measures of shape focus on eliminating effects largely of size and orientation (Wentz, 2000; Williams and Wentz, 2008). Wentz (2000) reviews a number of shape indices and presents a quantitative, trivariate definition of shape: *edge roughness*, *perforation*, and *elongation*. The edge roughness metric quantifies the nature of a feature by comparing its perimeter to its area. Perforation investigates the area of islands in defined shapes. Often, when investigating vector data, a feature will appear to have a hole, or an island completely contained within the feature. Perforation compares the area of the hole to the total area of the feature. The third index, elongation, describes deviation of a feature from a standard shape. Lee and Sallee (1970) first used elongation to describe different shapes of Sudanese villages. This method

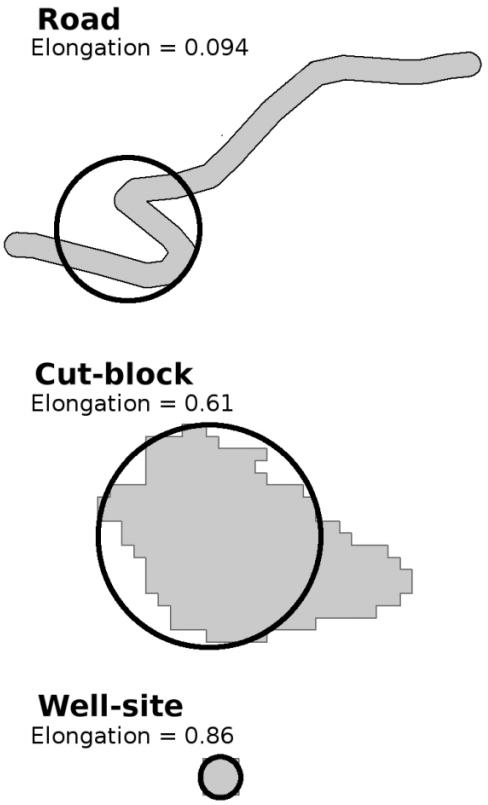

Figure 1. Example of the elongation metric as calculated on three disturbance types.

used four shapes, namely a circle, a rectangle, a square, and a triangle, to estimate the shape of the villages. Wentz took the same concept and made it more mathematically rigorous by describing the approximation shape as a circle of area equal to that of the geographic shape. The circle is then placed on the geographic shape where it will have maximum overlap, and the union of the two shapes is compared with the area of the shape by itself; this is the elongation index. **Figure 1** presents a graphical depiction and comparison of elongation values over different shape types.

Methods

Study area

Our study area is located in west-central Alberta, Canada, on the eastern slopes of the Rocky Mountains near the towns of Hinton and Edson (52°15′N, 116°30′W; **Figure 2**). The study area covers a wide elevation range (600–3900 m), with the natural subregion classified as upper foothills (Achuff, 1994). Forestry activities are well established and are the primary forest disturbance in the region, with fire less common due to ongoing suppression activities (Rhemtulla et al., 2002; Tande, 1979). Resource utilization activities, such as oil and gas extraction and mining, are also undertaken in the region (Schneider et al., 2003).

The study area is characterized using two image data sources, described in more detail below. A Landsat image is used to serve as a calibration (control) disturbance dataset and covers an area of 50 000 km^2, based on the Landsat image extent of 185 km × 185 km. An IRS-1C image covering 1050 km^2, based on an image extent of 30 km × 35 km, serves to provide higher spatial resolution information in support of the procedure applied. The study area is composed largely of closed conifer forest (52% of the control dataset study area), characterized by lodgepole pine (*Pinus contorta*) with species of spruce (*Picea glauca*, *Picea mariana*, and *Picea engelmannii*). Minor areas of trembling aspen (*Populus tremuloides*) or balsam poplar (*Populus balsamifera*) are also scattered throughout the area.

Data

The disturbance datasets were derived from two Landsat-7 Enhanced Thematic Mapper Plus (ETM+) images (path 44 and row 23 dated 19 October 1999 and 27 September 2000). The images were converted to at-satellite reflectance following Chander and Markham (2003). Following normalization, a tasselled cap transformation (Huang et al., 2002; Kauth and Thomas, 1976) was performed on both Landsat images (Han et al., 2007), with the resulting six bands used for both disturbance detection and rule-based attribution. Indian Remote Sensing (IRS) satellite imagery was used for higher resolution edge detection. An orthorectified 5.8 m panchromatic image was acquired on 31 May 2000. Cubic convolution resampling was applied with the resultant spatial resolutions of 30 m for the Landsat images and 5 m for the IRS-1C images.

Road network and digital elevation data were obtained from GeoBase (www.geobase.ca) for the province of Alberta (as provided by the Alberta Geomatics Section). The road network was used to determine both the distance between disturbance features and roads and the overlap of disturbance features and roads (termed percent road cover). These attributes were used in the classification model that was applied to the raw disturbance changes.

A detailed disturbance dataset was utilized to support the development of classification decision rules and to verify disturbance identification and labelling outcomes. The control disturbance dataset was developed through a combination of remote sensing, spatial data integration, and manual interpretation. A segmentation-based change detection protocol was implemented to define change regions representing cut blocks, burns, and mines based on greenness and the spectral bands from the Landsat images. Well sites were derived from a geographic information system (GIS) database as point features and visually verified against the temporally coincident imagery. Continuous road features were manually digitized from the Landsat imagery. The object accuracy was assessed against aerial photography. Additional detail on this control disturbance dataset and related methods can be found in Linke et al. (2009).

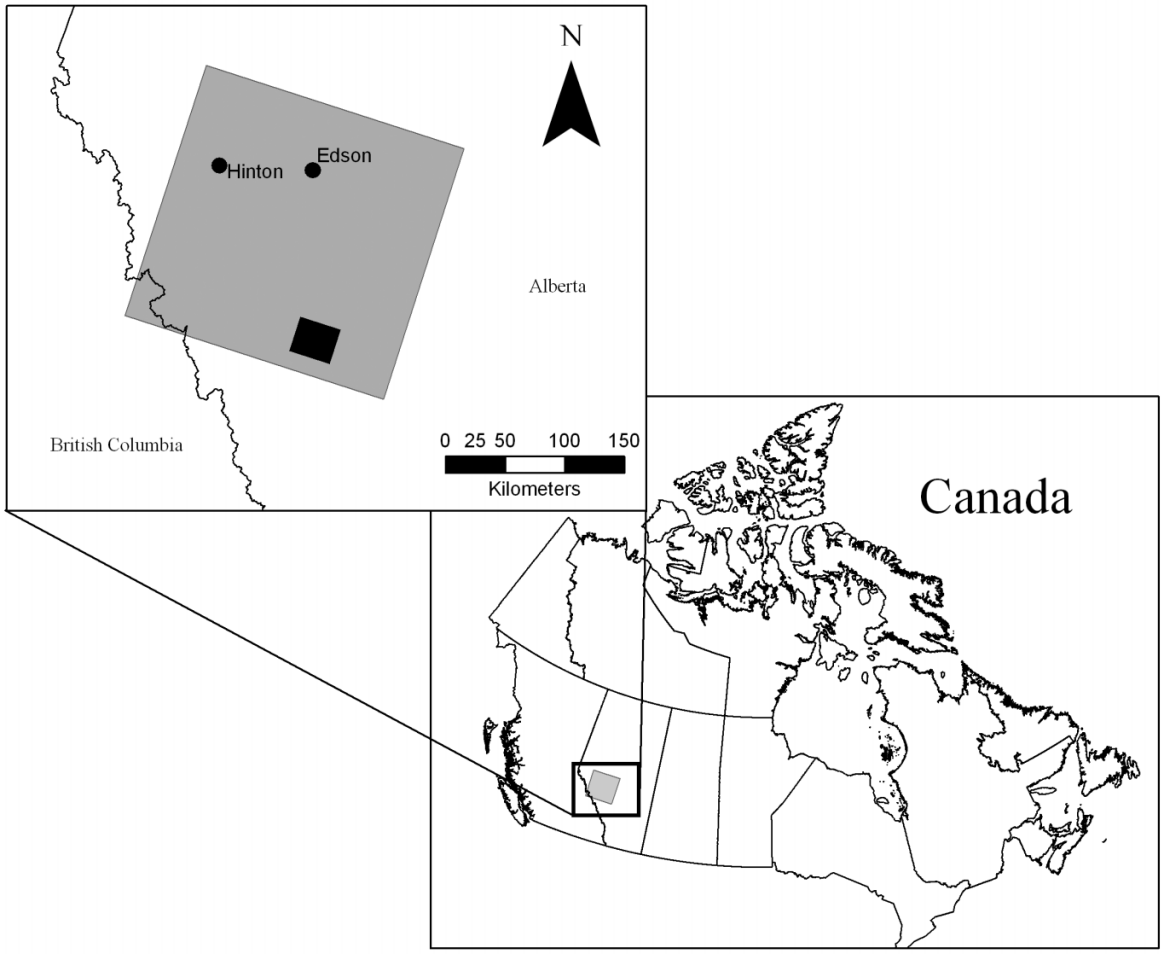

Figure 2. Study area located in west-central Alberta, Canada, occupying Landsat path 45 and row 23. The small black footprint indicates the area of the IRS-1C satellite image used to clean the EWDI changes.

Change detection

Following coregistration and normalization of the multitemporal Landsat images, the initial step in the automatic change detection and attribution procedure was to detect the location of disturbances via a threshold-based change detection technique (see workflow in **Figure 3**). The wetness bands of the tasselled cap transformation were differenced, resulting in an enhanced wetness difference index (EWDI) (Franklin et al., 2001; Skakun et al., 2003). The resulting EWDI was thresholded, as in Skakun et al. (2003), to partition change areas from no-change areas. The resultant change dataset (termed raw disturbances) was further refined using edge detection.

Edge detection

The second step in the automated change detection and attribution framework employs high spatial resolution imagery and edge detection to refine changes in the raw disturbances dataset that are linear in nature. To achieve this, edges were extracted from panchromatic IRS-1C imagery (5 m spatial resolution) using wombling. Wombling is an edge-detection technique that extracts edges based on their strength and direction (Womble, 1951; Barbujani et al., 1989; Fortin, 1994; 1997). Once extracted, these edges were used to classify raw disturbances as either noise or valid linear changes. Two metrics were calculated for all wombled edges that intersected changes detected in the EWDI. First, the distance between the changes along each detected edge was calculated. Second, the total area of change was compared with the total area of the edge, whereby edges extracted from the remotely sensed data maintained a minimum width of one pixel. If changes were found to be too far apart, or the area of the edge was much greater than the area of change, changes were discarded. Otherwise, changes were merged with the edge and were added to the extracted areal features for attribution (see **Figure 4** for an example).

Change attribution

The classification model used to attribute the raw disturbances incorporates shape-based attributes, contextual information concerning location relative to landscape

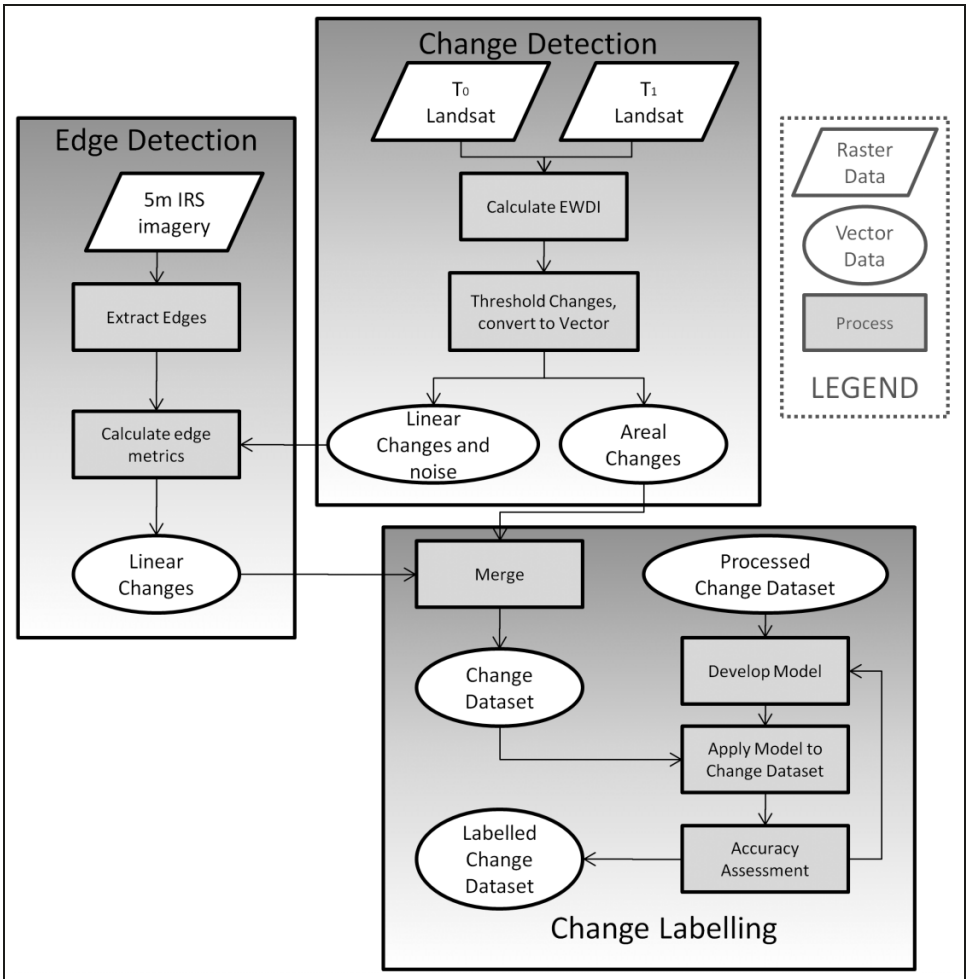

Figure 3. Workflow of change extraction and attribution framework. The process has three general steps: change extraction, edge detection, and change labelling.

Figure 4. Example of application of high-resolution images to medium-resolution changes. Black indicates changes detected in the EWDI, and gray indicates edges detected in the high-resolution imagery. Distance defines the average distance between changes on the linear feature, and area ratio is the ratio of linear area to change area. The left feature is classified as a real change, and the right is not.

Table 1. Attributes used in classification of disturbance features.

Attribute	Type	Description	Reference
T1 band means	Spectral reflectance	The average reflectance value for each band in the Landsat images was calculated for each disturbance feature	Weismiller et al., 1977; Jensen, 1986; Gong et al., 1992
Landsat band differences	Spectral reflectance	Difference between the T0 and T1 band values as calculated for each disturbance	
TCT values for T1	Composite values	Tasselled cap transformation (TCT) values calculated for all disturbance features, for each TCT value (brightness, greenness, wetness)	
TCT differences	Composite Values	Difference between the TCT values for the two Landsat images	
Shape area	Shape-based	Area of the disturbance feature	Williams, 2007; Xia, 1996
Shape perimeter	Shape-based	Perimeter of the disturbance feature	Xia, 1996
Shape elongation	Shape-based	EI = (area of intersection)/(area of union), where EI is the maximum overlap of the intersection and union of the disturbance feature with a circle of equal area	Wentz, 2000; Zhao and Stough, 2005
Edge roughness	Shape-based	Ed = [2 + log(perimeter)]/log(area) (this is ignored for shapes with an area of 1, but that did not occur in this dataset)	Wentz, 2000
Edge count	Shape-based	Number of edges of the disturbance	Hese and Schmullius, 2006
Distance to road	Shape-based	Linear distance to nearest road	Hese and Schmullius, 2006
Percent road cover	Shape-based	Percentage of the length of a feature that covers a part of the road network	

Note: T0 refers to the Landsat image obtained prior to the change detection, and T1 to the image after the disturbances.

Table 2. Accuracy of model classification on control dataset using cross-validation.

		Accuracy (%)			
	Kappa	All features (N = 1274)	Harvest areas (N = 561)	Roads (N = 267)	Well sites (N = 446)
All attributes	0.818	88.43	91.37	73.61	93.81
Shapes	0.788	86.48	88.30	70.14	94.17
Reflectance	0.643	77.21	88.20	56.46	76.03

Note: Cohen's kappa was calculated on the classification of all features. N, number of features.

objects, and reflectance values from the related Landsat and tasselled cap channels. **Table 1** presents a detailed list of all variables used in the classification. Spectral reflectance and composite band values were obtained by overlaying disturbance features over Landsat and composite band raster images. Elongation, edge roughness, and perforation were calculated for each disturbance feature and recorded for use in later calculations. The other shape-based attributes are single-parameter measures and were calculated using standard GIS operations.

Three classification models were generated using classification tree analysis. Models were based on the control dataset, and cross-validation was used to evaluate accuracy. Cross-validation was performed 100 times, with a random 75% of the disturbances used to train the model and the remaining 25% used for validation (random sampling was done without replacement). The first model was developed using only the spectral reflectance attributes, and the second model was based on shape-based attributes only. The third classification model was developed from both spectral and shape-based attributes. All classification models were developed via classification and regression tree analysis using the *rpart* package (Therneau et al., 2008) of the R 2.7.2 software package (www.r-project.org). The splitting algorithm is based on Breiman et al. (1984); default splitting values were used (related to node size, minimum bucket size, and complexity parameter), and no pruning was performed. The three models were compared to determine if shape-based attributes proved useful in the classification of remotely sensed disturbance features. The model containing both shape and reflectance metrics was then used to attribute the raw change dataset extracted from the EWDI. The attributed raw disturbances were compared to the definitions from the control disturbance dataset to compute accuracies and compare areas of correctly labelled disturbances. Both percent accuracy and Cohen's kappa were calculated to assess model accuracy (Cohen, 1960). The classification tree model is developed using support information from the entire Landsat image area. The application is made on the overlapping area between the IRS and Landsat imagery, 1050 km^2, as noted previously.

Results

Three classification models were created based on the control disturbance dataset. One model was based on all attributes, one only on shape attributes, and one only on reflectance attributes. **Table 2** lists the disturbance counts,

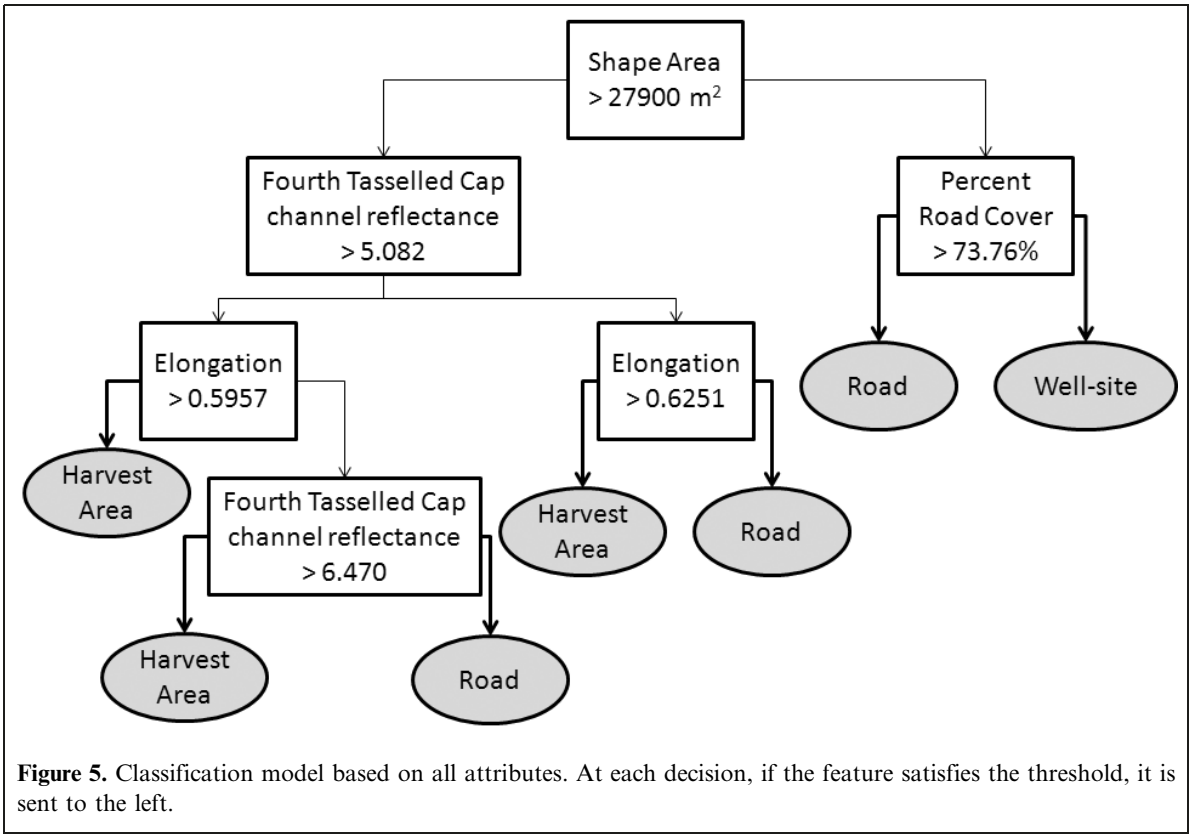

Figure 5. Classification model based on all attributes. At each decision, if the feature satisfies the threshold, it is sent to the left.

accuracy, and kappa values of each model, averaged over the 100 iterations supporting the validation. The model with all attributes performed best in all categories, with an overall accuracy of 88% and a kappa value of 0.82. The shape-based model outperformed the reflectance-based model, with an accuracy and kappa value of 86% and 0.79, respectively, compared with 77% and 0.64 for the reflectance model. Road disturbances had the lowest predictive success, with the all-attributes model accurately attributing 73%, whereas the reflectance model only attributed 56% correctly.

An example of the classification model generated through our tree splitting algorithm is shown in **Figure 5** and represents the most accurate model, based on all attributes. The model shows a combination of shape- and reflectance-based attributes. The primary split is based on shape area, with large shapes (left side) separated by the fourth band of the tasselled cap transformation and small shapes separated based on percent road cover. Further classification is performed on large shapes, based on elongation, and again on the fourth tasselled cap channel.

Raw disturbances were extracted from the EWDI following the development of our classification model. The disturbances were refined using edge features extracted from the IRS-1C image; see **Table 3** for a breakdown of the differences between the control and raw disturbances. Of the 75 disturbance features in the control dataset that are found in the IRS-1C study area, 57 were detected. Of the 61 raw disturbance features detected through our automatic framework, 60 correspond to disturbances in the control dataset. Overall, 77% of the disturbances in the control dataset were found using automatic change detection. However, 91% of the area of change in the control dataset is found through the automatic framework (92% of the harvest areas, 90% of the road features, and 100% of the well sites).

Figure 6 provides examples of disturbance mismatches in the 5 m panchromatic IRS image. The black polygon on the

Table 3. Accuracy of disturbance detection through automatic detection approach (limited to common area between the Landsat and IRS-1C images, as shown in **Figure 2**).

	Control		Agreement to mapped		Omission		Commission	
	N	Area (m^2)	*N*	Area (m^2)	*N*	Area (m^2)	*N*	Area (m^2)
Harvest area	51	8 869 499	45	8 126 099	6	743 400	0	—
Road	22	5 647 473	13	5 078 272	8	569 201	1	101 296
Well site	2	23 400	2	23 400	0	—	0	—

Note: *N*, number of change features.

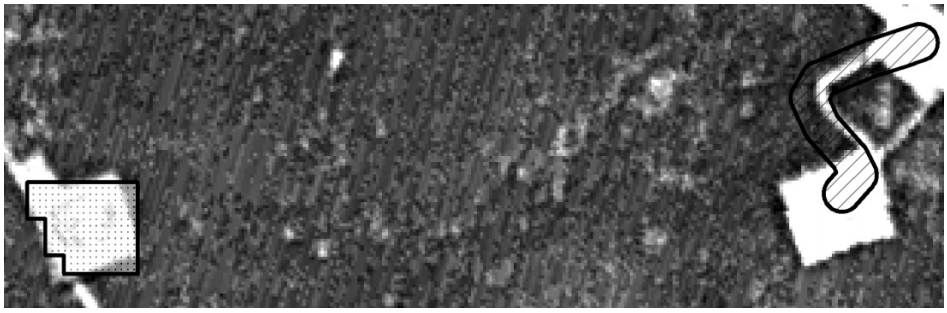

Figure 6. Example of detected and not detected changes. The black outline indicates a well site that was successfully detected and labelled through our automatic framework. The gray road was present in the control dataset but was missed in the automatic framework.

Table 4. Accuracy of classification of and labelling of disturbances using all-attributes model (includes only those features identified in the automatic change detection).

	Accuracy (%)			
Kappa	All features (N = 61)	Harvest areas (N = 45)	Roads (N = 14)	Well sites (N = 2)
0.868	91.11	92.35	72.03	100.00

left side in **Figure 6** is a disturbance that was detected via the EWDI change detection and correctly identified as a well site via the attribution framework. The polygon on the right side in **Figure 6** represents a short road that was not identified via the EWDI change detection due to its proximity to two other bright disturbances and its size and shape (i.e., short and narrow).

Raw changes were attributed with disturbance type based on the classification model developed from the control dataset and compared to the disturbance label from the control dataset. The overall accuracy was 91% when classifying raw disturbance features, with a kappa value of 0.87 (see **Table 4**). All three disturbance types showed high classification accuracy, with harvest areas showing an accuracy of 91% and roads and well sites showing accuracies of 72% and 100%, respectively.

Discussion

The creation of an automated change detection and attribution framework is intended to reduce subjectivity and improve timeliness of change detection and attribution. Since most change detection relies on remotely sensed data, the incorporation of GIS-based shape and contextual attributes has added an additional dimension to our classification. Evidence for the importance of these metrics is seen in the comparison of the three classification models (shape-based, reflectance-based, and all attributes). The reflectance-only model correctly attributed only 77% of the disturbance features and 56% of the road features. The model containing all attributes accurately labelled 88% of all features and 72% of the road features. The model with all attributes contains both shape and reflectance attributes, highlighting the importance of both types of metrics in differentiating disturbances.

The second aspect of this classification, namely the extraction and attribution of disturbance features, yields equally encouraging results. The incorporation of high spatial resolution imagery to traditional EWDI change detection allows us much greater confidence in the accuracy of our change detection, specifically for linear features. Previous studies have shown that extraction of road features from Landsat-based imagery is problematic (Klang, 1998; Zhang et al., 2002), especially when considering narrow or short roads, such as those associated with logging and resource extraction. Although our change detection methods identified 45 of 51 harvest areas and all of the well sites, just over half (13 of 22) of the road features were identified. When considering the area of the detected changes, it is evident that although half of the individual road features are missed, 90% of the area of road features is captured using our approach. This indicates that small, short roads are missed, similar to that indicated in **Figure 6**. Although these disturbances can play an important role in ecological modelling, many of these roads connect harvest areas and are often included in the harvest areas captured. Errors of omission (found in control, absent in raw changes) were present in our study; however, errors of commission (raw changes not found in control) were minor. This is expected, as the change detection used for the control dataset and the automatic framework both incorporate change in Landsat-derived tasselled cap transformations. The errors of omission stem from manually digitized features in the control dataset not appearing in Landsat imagery, typically small, short roads near other disturbance features. The lack of commission error indicates the stability of tasselled cap difference derived change detection approaches. The demonstrated ability of the approach to find the changes of interest in reference to the control dataset allows us to focus on the attribution of change type. The transparent and rigorously developed labelling of the change features in the control change layer is of importance to this study, as

this provides us with the capacity to both train a classifier and ascertain the quality of our results (with an independent subset). Overall, a 91% agreement between the control dataset and the change attribution approach was found, although linear features were less accurately captured and attributed on a class-specific basis (72% agreement). This indicates we have developed an approach that can be implemented to detect and then attribute a range of disturbance features, thereby reducing reliance on human intervention, especially for area-based change features such as forest harvesting. We anticipate that there will be an ongoing need to improve our detection and attribution methods for linear features or other features that are subpixel in extent or width. Further, we acknowledge the difficulties in integrating the multiscale image datasets. Alberta is an ideal test bed for methods such as this due to the periodic collection there of province-wide IRS image coverage. Even with the wide-area coverage, the vintage of the imagery must also be considered. We feel that a strength of the approach presented is that we do not expect all the sub-Landsat pixel features to be mapped perfectly and in entirety. We consider the information from the IRS imagery to provide additional information to support the mapping undertaken with the Landsat imagery. In so doing, we are able to adjust the rules applied when integrating the IRS edge features with the Landsat change features. In moving towards an operational implementation of an approach such as this, we are encouraged by the growing number of high spatial resolution satellite systems and the inclusion of higher spatial resolution panchromatic channels on multispectral optical satellites. With the open access to the Landsat archive (Woodcock et al., 2008), opportunities for use of archived higher spatial resolution images also exist, although the opening of the Landsat archive and an interest in integrating differing data types may also serve to highlight that most other satellites do not have systematic collection or archiving procedures to support the desired analysis. Commercial satellite operators and vendors, such as DigitalGlobe, are increasingly collecting data to enable wide-area coverage and population of a searchable archive (with partner Google). Although the approximate 10 km $\times$ 10 km footprint of these very high spatial resolution sensors will be of limited utility for application of the approach presented here, it is the increasing interest in collecting data systematically and archiving that is the promising development.

Conclusion

We have developed an approach for effectively extracting disturbances using medium spatial resolution imagery in concert with edges extracted from high spatial resolution imagery. A classification model was developed from a disturbance dataset that had been manually cleaned and digitized with carefully labelled point and line features. This model was used to classify disturbance features that were attributed with disturbance type based on their shape and reflectance attributes. An overall accuracy of 91% was achieved in automatically detecting and attributing disturbance features.

By automatically detecting and then attributing changes, operational procedures for monitoring can be developed to facilitate large area classification efforts. With the recent release of the Landsat archive for free public consumption (Woodcock et al., 2008), there is a wealth of historical imagery that may be utilized. Although we acknowledge that IRS-1C data may not always be available for the desired locations or time periods, these types of high spatial resolution data are becoming increasingly available. Approaches such as that demonstrated here provide additional options for operationally observing land use and land cover change with remotely sensed data.

Acknowledgments

Funding for this research was generously provided by the Grizzly Bear Program of the Foothills Research Institute located in Hinton, Alberta, Canada (additional information available at www.fmf.ab.ca/); Alberta Science and Innovation; and the Natural Sciences and Engineering Research Council of Canada. We thank Julia Linke for assistance with data processing and research design. Michael J. Falkowski, formerly of the Canadian Forest Service and currently of the Michigan Technological University, is thanked for inputs to an earlier draft of this manuscript. Samuel Alan Stewart is thanked for his assistance in data processing and statistical analysis. Much of the Landsat data used in this study were contributed by the US Geological Survey Landsat Data Continuity Mission Project through participation of Wulder on the Landsat Science Team.

References

Achuff, P.L. 1994. *Natural regions, subregions and natural history themes of Alberta: A classification for protected areas management*. Alberta Environmental Protection, Edmonton, Alta. 72 pp.

Archibald, W.R., Ellis, R., and Hamilton, A.N. 1987. Responses of grizzly bears to logging truck traffic in the Kimsquit River Valley, British Columbia. *Bears: Their Biology and Management*, Vol. 7, No. 1, pp. 251–257.

Barbujani, G., Oden, N.L., and Sokal, R.R. 1989. Detecting regions of abrupt change in maps of biological variables. *Systematic Zoology*, Vol. 38, No. 4, pp. 376–389.

Breiman, L., Friedman, J.H., Olshen, R.A., and Stone, C.J. 1984. *Classification and regression trees.* Wadsworth Inc., Belmont, Calif. 358 pp.

Chander, G., and Markham, B. 2003. Revised Landsat-5 TM radiometric calibration procedures and postcalibration dynamic ranges. *IEEE Transactions on Geoscience and Remote Sensing*, Vol. 41, No. 11, pp. 2674–2677.

Cohen, J. 1960. A coefficient of agreement for nominal scales. *Educational and Psychological Measurement*, Vol. 41, pp. 687–699.

Cohen, W.B., Fiorella, M., Gray, J., Helmer, E., and Anderson, K. 1998. An efficient and accurate method for mapping forest clearcuts in the Pacific Northwest using Landsat imagery. *Photogrammetric Engineering & Remote Sensing*, Vol. 64, No. 4, pp. 293–300.

Cohen, W., Spies, T., Alig, R., Oetter, D., Maiersperger, T., and Fiorella, M. 2002. Characterizing 23 years (1972–95) of stand replacement disturbance in western Oregon forests with Landsat imagery. *Ecosystems*, Vol. 5, No. 2, pp. 122–137.

Coppin, P., and Bauer, M. 1996. Change detection in forest ecosystems with remote sensing digital imagery. *Remote Sensing Reviews*, Vol. 13, pp. 207–234.

Coppin, P., Jonckheere, I., Nackaerts, K., and Muys, B. 2004. Digital change detection methods in ecosystem monitoring: a review. *International Journal of Remote Sensing*, Vol. 25, No. 9, pp. 1565–1596.

Culvenor, D.S. 2003. Survey of techniques for extracting individual tree information from high spatial resolution imagery. In *Remote sensing of forest environments: concepts and case studies*. Edited by M.A. Wulder and S.E. Franklin. Kluwer Academic Publishers, Boston, Mass. Chapt. 9, pp. 225–279.

Desclee, B., de Wasseige, C., Bogaert, P., and Defourny, P. 2006. Tropical forest monitoring by object-based change detection: towards an automated method in an operational perspective. In *OBIA 2006: Proceedings of the 1st International Conference on Object-based Image Analysis*, 4–5 July 2006, Salzburg, Austria. Edited by S. Lang, T. Blaschke, and E. Schöpfer. ISPRS Volume XXXVI-4/C42, ISPRS, Enschede, The Netherlands [www.commission4.isprs.org/obia06].

Fortin, M.-J. 1994. Edge detection algorithms for two-dimensional ecological data. *Ecology*, Vol. 75, No. 4, pp. 956–965.

Fortin, M.-J. 1997. Effects of data types on vegetation boundary delineation. *Canadian Journal of Forest Research*, Vol. 27, No. 11, pp. 1851–1858.

Franklin, S., Lavigne, M., Moskal, M., Wulder, M., and McCaffrey, T.M. 2001. Interpretation of forest harvest conditions in New Brunswick using Landsat TM enhanced wetness difference imagery (EWDI). *Canadian Journal of Remote Sensing*, Vol. 27, No. 1, pp. 118–128.

Frohn, R.C. 2006. The use of landscape pattern metrics in remote sensing image classification. *International Journal of Remote Sensing*, Vol. 27, No. 10, pp. 2025–2032.

Fung, T., and LeDrew, E.F. 1988. The determination of optimal threshold levels for change detection using various accuracy indices. *Photogrammetric Engineering & Remote Sensing*, Vol. 54, No. 10, pp. 1449–1454.

Gong, P., LeDrew, E.F., and Miller, J.R. 1992. Registration-noise reduction in difference images for change detection. *International Journal of Remote Sensing*, Vol. 13, No. 4, pp. 773–779.

Häme, T., Heiler, I., and San Miguel-Ayanz, J. 1998. An unsupervised change detection and recognition system for forestry. *International Journal of Remote Sensing*, Vol. 19, No. 6, pp. 1079–1099.

Han, T., Wulder, M.A., White, J.C., Coops, N.C., Alvarez, M.F., and Butson, C. 2007. An efficient protocol to process Landsat images for change detection with Tasselled Cap Transformation. *Geoscience and Remote Sensing Letters*, Vol. 4, No. 1, pp. 147–151.

Hayes, D.J., and Sader, S.A. 2001. Comparison of change-detection techniques for monitoring tropical forest clearing and vegetation regrowth in a time series. *Photogrammetric Engineering & Remote Sensing*, Vol. 67, No. 9, pp. 1067–1075.

Hese, S., and Schmullius, C. 2006. Object context information for advanced forest change classification strategies. In *OBIA 2006: Proceedings of the 1st International Conference on Object-based Image Analysis*, 4–5 July 2006, Salzburg, Austria. Edited by S. Lang, T. Blaschke, and E. Schöpfer. ISPRS Volume XXXVI-4/C42, ISPRS, Enschede, The Netherlands [www.commission4.isprs.org/obia06].

Huang, C., Wylie, B., Yang, L., Homer, C., and Zylstra, G. 2002. Derivation of a tasselled cap transformation based on Landsat 7 at-satellite reflectance. *International Journal of Remote Sensing*, Vol. 23, No. 8, pp. 1741–1748.

Hyyppa, J., Hyyppa, H., Inkinen, M., Engdahl, M., Linko, S., and Zhu, Y.-H. 2000. Accuracy comparison of various remote sensing data sources in the retrieval of forest stand attributes. *Forest Ecology and Management*, Vol. 128, No. 1, pp. 109–120.

Jensen, J. 1986. *Introductory digital processing: a remote sensing perspective*. Prentice-Hall, Englewood Cliffs, N.J. 316 pp.

Kauth, R.J., and Thomas, G.S. 1976. The Tasselled Cap—A graphical description of the spectral–temporal development of agricultural crops as seen by LANDSAT. In *Proceedings of the Symposium on Machine Processing of Remotely Sensed Data*, 29 June – 1 July 1976, Purdue University, West Lafayette, Ind. IEEE, New York. pp. 41–51.

Klang, D. 1998. Automatic detection of changes in road databases using satellite imagery. *International Archives of Photogrammetry and Remote Sensing*, Vol. 32, No. 4, pp. 293–298.

Lee, D.R., and Sallee, G.T. 1970. A method of measuring shape. *Geographical Review*, Vol. 60, No. 4, pp. 555–563.

Lewis, H.G., Cote, S., and Tatnall, A.R.L. 1997. Determination of spatial and temporal characteristics as an aid to neural network cloud classification. *International Journal of Remote Sensing*, Vol. 18, No. 4, pp. 899–915.

Linke, J., Franklin, S.E., Hall-Beyer, M., and Stenhouse, G.B. 2008. Effects of cutline density and land-cover heterogeneity on landscape metrics in western Alberta. *Canadian Journal of Remote Sensing*, Vol. 34, No. 4, pp. 390–404.

Linke, J., McDermid, G.J., Laskin, D.N., McLane, A.J., Pape, A.D., Cranston, J., Hall-Beyer, M., and Franklin, S.E. 2009. A disturbance-inventory framework for flexible and reliable landscape monitoring. *Photogrammetric Engineering & Remote Sensing*, Vol. 75, No. 8, pp. 981–996.

Ludeke, A.K., Maggio, R.C., and Reid, L.M. 1990. An analysis of anthropogenic deforestation using logistic regression and GIS. *Environmental Management*, Vol. 31, No. 3, pp. 247–259.

Mace, R.D., Waller, J.S., Manley, T.L., Lyon, L.J., and Zuuring, H. 1996. Relationships among grizzly bears, roads and habitat in the Swan Mountains, Montana. *Journal of Applied Ecology*, Vol. 33, No. 6, pp. 1395–1404.

McFarlane, B.L., and Boxall, P.C. 2000. Factors influencing forest values and attitudes of two stakeholder groups: the case of the foothills model forest, Alberta, Canada. *Society & Natural Resources*, Vol. 13, No. 7, pp. 649–661.

Nielsen, S.E., Boyce, M.S., and Stenhouse, G.B. 2004. Grizzly bears and forestry: I. Selection of clearcuts by grizzly bears in west-central Alberta, Canada. *Forest Ecology and Management*, Vol. 199, No. 1 pp. 51–65.

Radke, R.J., Andra, S., Al-Kofahi, O., and Roysam, B. 2005. Image change detection algorithms: a systematic survey. *IEEE Transactions on Image Processing*, Vol. 14, No. 3, pp. 294–307.

Rhemtulla, J.M., Hall, R.J., Higgs, E.S., and Macdonald, S.E. 2002. Eighty years of change: vegetation in the montane ecoregion of Jasper National Park, Alberta, Canada. *Canadian Journal of Forest Research*, Vol. 32, No. 11, pp. 2010–2021.

Schneider, R.R., Stelfox, J.B., Boutin, S., and Wasel, S. 2003. Managing the cumulative impacts of land uses in the Western Canadian Sedimentary Basin: a modeling approach. *Conservation Ecology*, Vol. 7, No. 1, p. 8.

Skakun, R., Wulder, M., and Franklin, S. 2003. Sensitivity of the thematic mapper enhanced wetness difference index to detect mountain pine beetle red-attack damage. *Remote Sensing of Environment*, Vol. 86, No. 4, pp. 433–443.

Tande, G.F. 1979. Fire history and vegetation pattern of coniferous forests in Jasper National Park, Alberta. *Canadian Journal of Botany*, Vol. 57, No. 18, pp. 247–259.

Therneau, T.M., Atkinson, B., and Ripley, B. 2008. *rpart: recursive partitioning*. R package version 3.1-42.

Weismiller, R., Kristof, S., Scholz, D., Anuta, P., and Momin, S. 1977. Change detection in coastal zone environments. *Photogrammetric Engineering & Remote Sensing*, Vol. 43, No. 1, pp. 1533–1539.

Wentz, E.A. 1997. Shape analysis in GIS. *Auto-Carto*, Vol. 13, No. 1, pp. 204–213.

Wentz, E.A. 2000. A shape definition for geographic applications based on edge, elongation, and perforation. *Geographical Analysis*, Vol. 32, No. 2, pp. 95–112.

Williams, E.A., and Wentz, E.A. 2008. Pattern analysis based on type, orientation, size, and shape. *Geographical Analysis*, Vol. 40, No. 2, pp. 97–122.

Womble, W.H. 1951. Differential systematics. *Science (Washington, D.C.)*, Vol. 114, No. 2961, pp. 315–322.

Woodcock, C.E., Macomber, S.A., Pax-Lenney, M., and Cohen, W.B. 2001. Monitoring large areas for forest change using Landsat: generalization across space, time and Landsat sensors. *Remote Sensing of Environment*, Vol. 78, No. 2, pp. 194–203.

Woodcock, C.E., Allen, R., Anderson, M., Belward, A., Bindschadler, R., Cohen, W., Gao, F., Goward, S.N., Helder, D., Helmer, E., Nemani, R., Oreopoulos, L., Schott, J., Thenkabail, P.S., Vermote, E.F., Vogelmann, J., Wulder, M.A., and Wynne, R. 2008. Free access to Landsat imagery. *Science (Washington, D.C.)*, Vol. 320, No. 5879, p. 1011.

Wulder, M.A., White, J.C., Goward, S.N., Masek, J.G., Irons, J.R., Herold, M., Cohen, W.B., Loveland, T.R., and Woodcock, C.E. 2008. Landsat continuity: Issues and opportunities for land cover monitoring. *Remote Sensing of Environment*, Vol. 112, No. 3, pp. 955–969.

Zager, P., Jonkel, C., and Habeck, J. 1983. Logging and wildfire influence on Grizzly Bear habitat in northwestern Montana. *Bears: Their Biology and Management*, Vol. 5, No. 1, pp. 124–132.

Zhang, Q., Wang, J., Peng, X., Gong, P., and Shi, P. 2002. Urban built-up land change detection with road density and spectral information from multi-temporal Landsat TM data. *International Journal of Remote Sensing*, Vol. 23, No. 15, pp. 3057–3078.

Zhao, Z., and Stough, R. 2005. Measuring similarity among various shapes based on geometric matching. *Geographical Analysis*, Vol. 37, No. 4, pp. 410–422.